Supporting Information

Strong exciton-plasmon coupling in WS$_2$ monolayer on Au film

hybrid structures mediated by liquid Ga nanoparticles

Fu Deng[1], Hongfeng Liu[1], Lei Xu[2], Sheng Lan[1] [*] and Andrey E. Miroshnichenko[2] [*]

[1] Guangdong Provincial Key Laboratory of Nanophotonic Functional Materials and Devices, School of Information and Optoelectronic Science and Engineering, South China Normal University, Guangzhou 510006, China
[2] School of Engineering and Information Technology, University of New South Wales, Canberra, ACT 2600, Australia
*Corresponding author: slan@scnu.edu.cn; andrey.miroshnichenko@unsw.edu.au

S1: SEM image of WS$_2$ monolayer

The SEM image of a typical WS$_2$ monolayer placed on a thin Au film used in our study is shown in Figure S1.
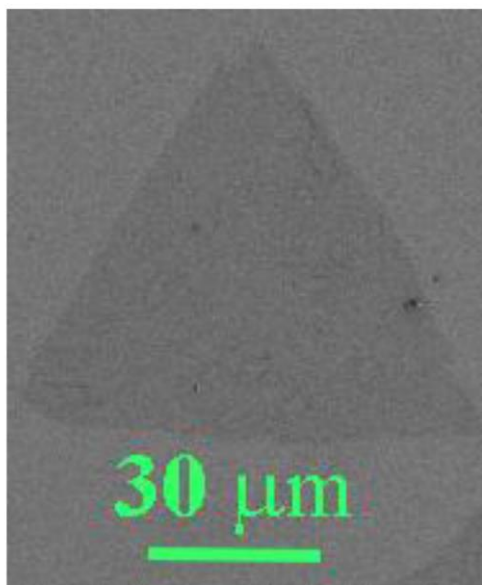

Figure S1. SEM image of a WS$_2$ monolayer placed on a thin Au film used in our study.

S2: Detailed configuration for numerical simulation

 The detailed configuration for simulating the reflection spectra presented in Figure 1 is shown in the following. The numerical simulations were performed on a two-dimensional structure with Bloch periodic boundary conditions in the x direction and perfectly matched layers (PML) in the z direction to absorb the outgoing waves. The incident light is a TM-polarized plane wave with a broad spectrum. The monitor used to detect the reflected light is placed horizontally on top of the Au film (see Figure S2).
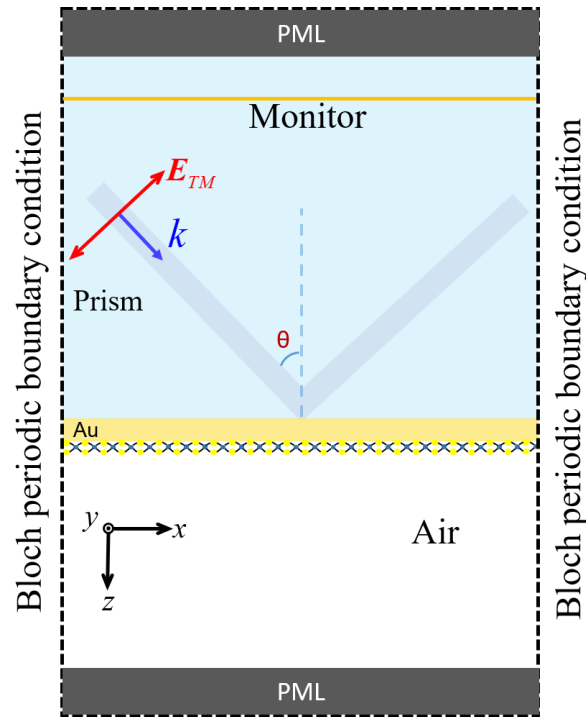
Figure S2. Detailed structure used to obtain the simulation results shown in Figure 1.

S3: Coupling of excitons in WS$_2$ and SPPs generated by Otto configuration

The schematic showing the coupling of the excitons in a WS$_2$ monolayer and the SPPs generated by using the Otto configuration is presented in Figure S3a. The reflection spectra of the WS$_2$/Au hybrid structure excited by a TM-polarized light incident at different angles are shown in Figures S3b and c. It is noticed that SPPs can be excited in this structure and the strong coupling can be realized. In this case, however, a dielectric layer with refractive index smaller than that of the prism is necessary. If the dielectric layer is removed, no SPPs can be excited, as can be seen from the reflection spectra shown in Figure S3d where only the absorption of the monolayer WS$_2$ is observed.
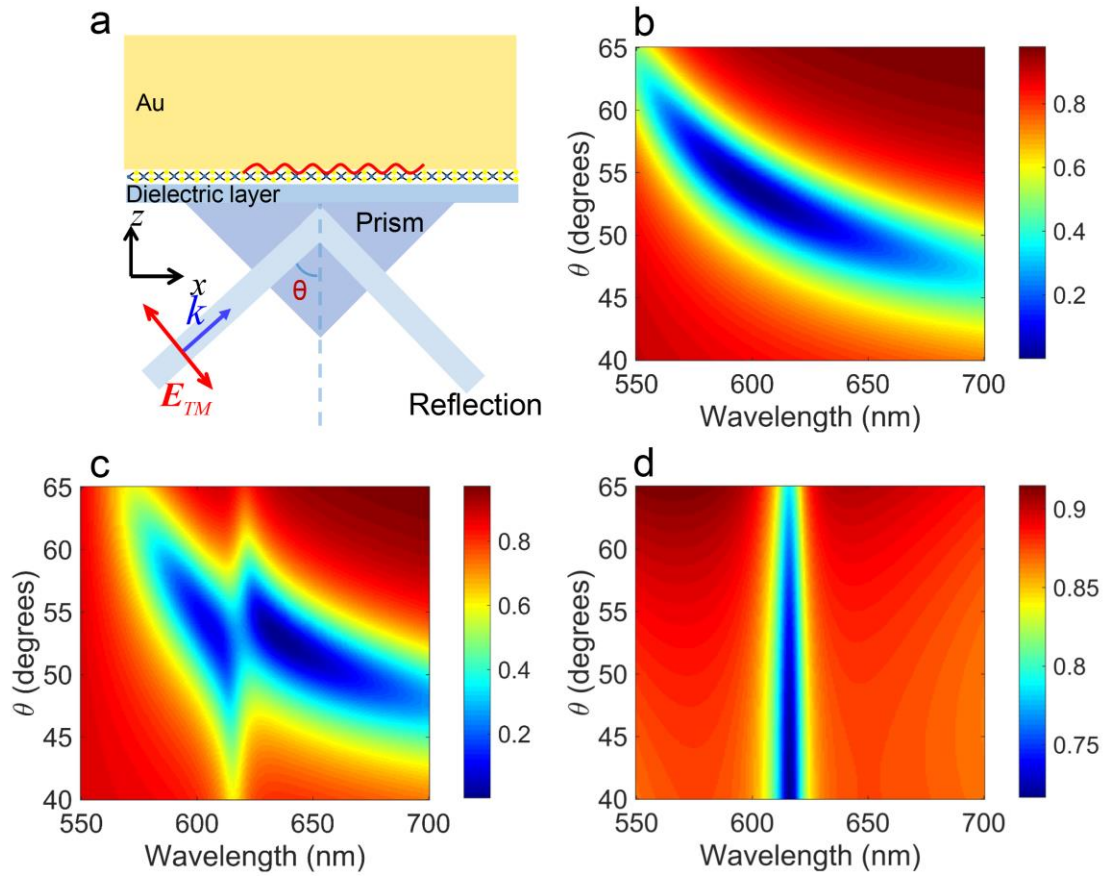

Figure S3. (a) Schematic showing of the excitation of SPPs on the surface of a WS$_2$/Au hybrid structure via the Otto configuration. (b) and (c) show the reflection spectra of the structure without and with a WS$_2$ monolayer. Parameters: $n_d = 2$ (refractive index of the dielectric layer), $t = 100$ nm (thickness of the dielectric layer), and $n_{prism} = 3.5$ (refractive index of the prism). (d) The reflection spectra of the structure without the dielectric layer.

S4: SPPs generated in the K-R configuration

The spectra of the reflected light from the Au film with increasing incidence angle measured in the K-R configuration are shown in Figure S4.
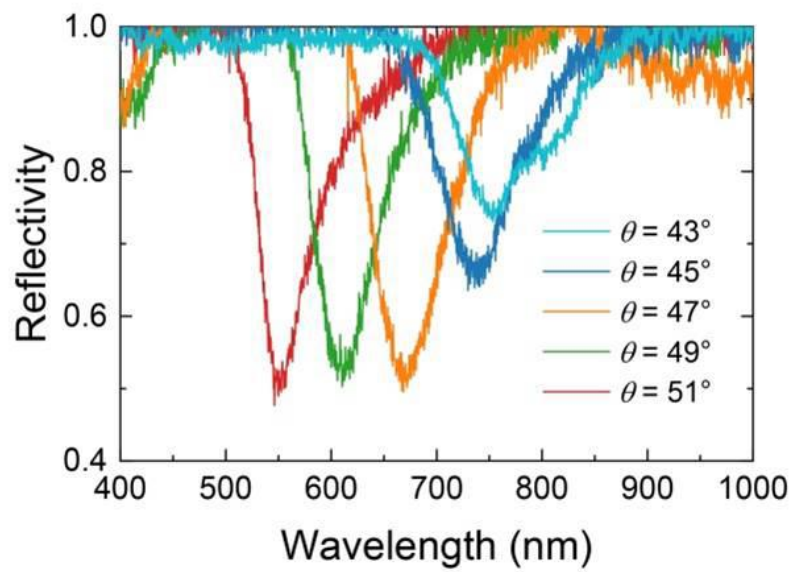

Figure S4. Spectra of the reflected light from the Au film with increasing incidence angle measured in the K-R configuration.

S5: Field distributions of nanoparticles on top of the Au film excited by SPPs

In Figure S5, we present the distribution of the x component of the electric field (E_x) calculated for a Ga nanoparticle and a dielectric nanoparticle with the same diameter ($d \sim 212.6$ nm) placed on a 50-nm-thick Au film. They are excited by using the SPPs generated via the K-R configuration. It is found that E_x can be enhanced by one order of magnitude if we choose the Ga nanoparticle instead of the dielectric nanoparticle with a refractive index of $n \sim 2$, such as polystyrene nanoparticle. Different from the dielectric nanoparticle where the maximum enhancement in E_x is found at the two sides of the dielectric nanoparticle, the maximum enhancement in E_x for the Ga nanoparticle is achieved in the gap region between the Ga nanoparticle and the Au film. This feature makes Ga nanoparticles a good candidate for boosting the interaction of the excitons in a WS_2 monolayer and the localized plasmons supported by the nanocavity composed of the Ga nanoparticle and the Au film.
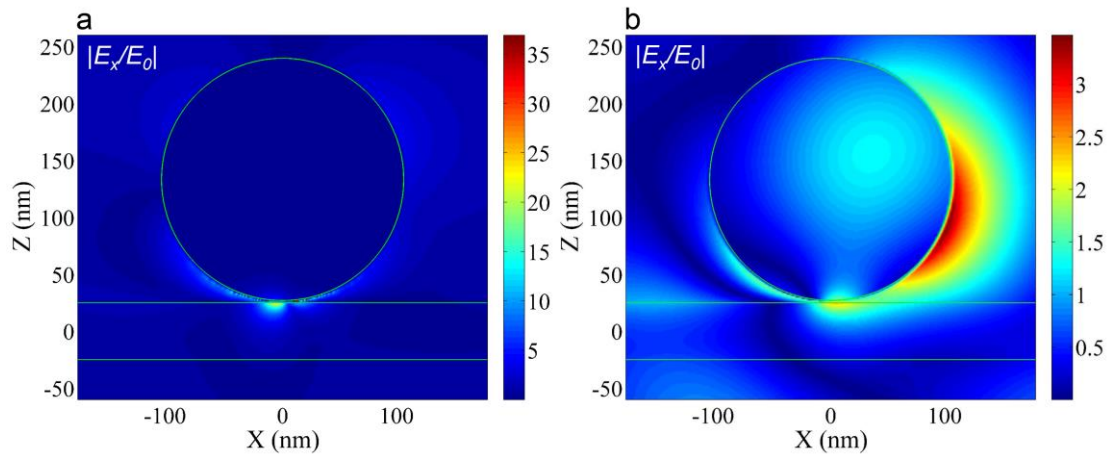

Figure S5. Distribution of the x component of the electric field (E_x) on the XZ plane calculated for a Ga nanoparticle (a) and a dielectric nanoparticle ($n_d = 2.0$) (b) with the same diameter of $d = 212.6$ nm placed on the Au film. In both cases, the gap between the nanoparticle and the Au film, the incidence angle and the wavelength of the incident light were chosen to be 1 nm, 46º, and 600 nm, respectively.

S6: Scattering imaging in our experiment

The image of the plasmonic nanocavities recorded by using a charge coupled device are shown in Figure S6. The Ga nanoparticle enclosed by the red circle is the one described in Figure 4a of the main text.
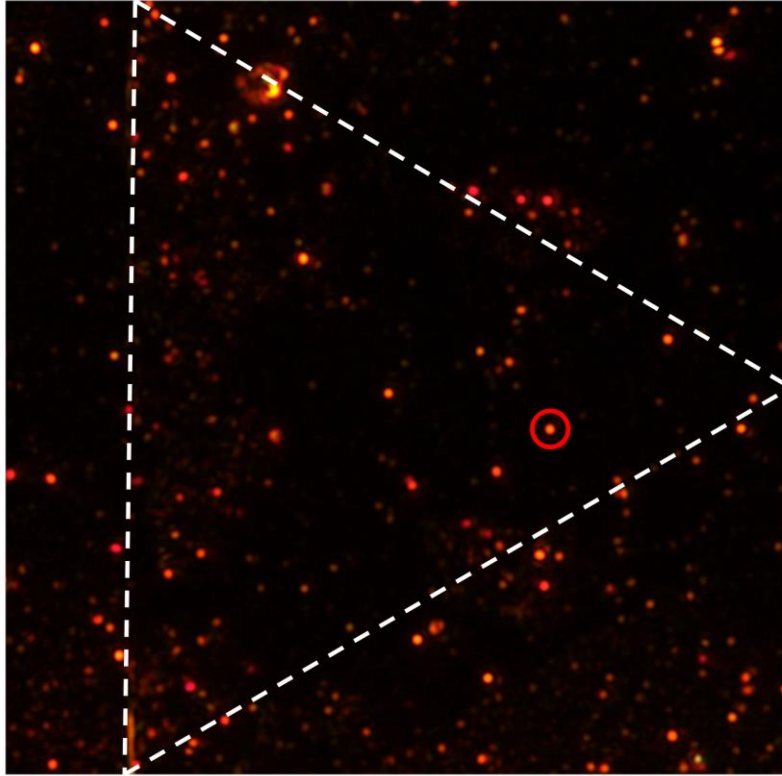

Figure S6. CCD image of the WS_2/Au hybrid structure excited by the SPPs generated at an incidence angle of 46°. The white triangle is the outline of the WS_2 monolayer. The red circle indicates the position of the Ga nanoparticle described in the main text.

S7: Electric field enhancement of the nano-cavity excited by an obliquely incident plane wave

We also calculated the distributions of the electric field (E_x and E_z) for the same plasmonic nanocavity excited by using a TM-polarized light incident at an angle of 46°, as shown in Figure S7. In this case, no SPPs are excited and the enhancement factor for E_z is much larger than that for E_x. It is noticed that the enhancement factor for E_x is only ~4.0, which is not suitable for studying and observing strong exciton-plasmon coupling with WS_2 monolayer.
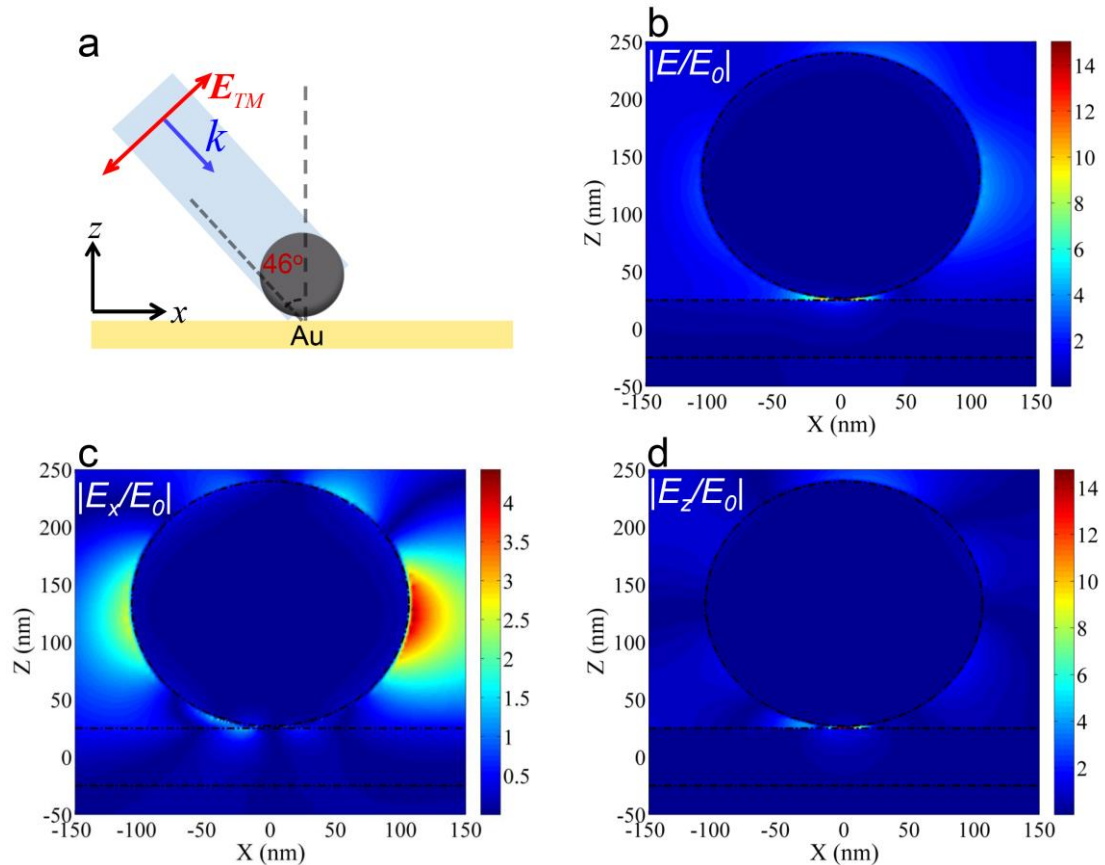

Figure S7. (a) Schematic showing of the nano-cavity excited by an obliquely incident plane wave. The distributions of the total electric field, the x component and the z component of the electric field are shown in (b), (c), and (d), respectively. The gap between the Ga nanoparticle and the Au film was set to be 1 nm.

S8: Scattering spectra measured for a Ga nanoparticle at different incidence angles without the WS$_2$ monolayer

In Figure S8, we present the scattering spectra measured for a Ga nanoparticle at different incidence angles without the WS$_2$ monolayer. In this case, the scattering spectra reflect the SPPs generated on the surface of the Au film and the resonant wavelength is shifted to shorter wavelengths with increasing the incidence angle.
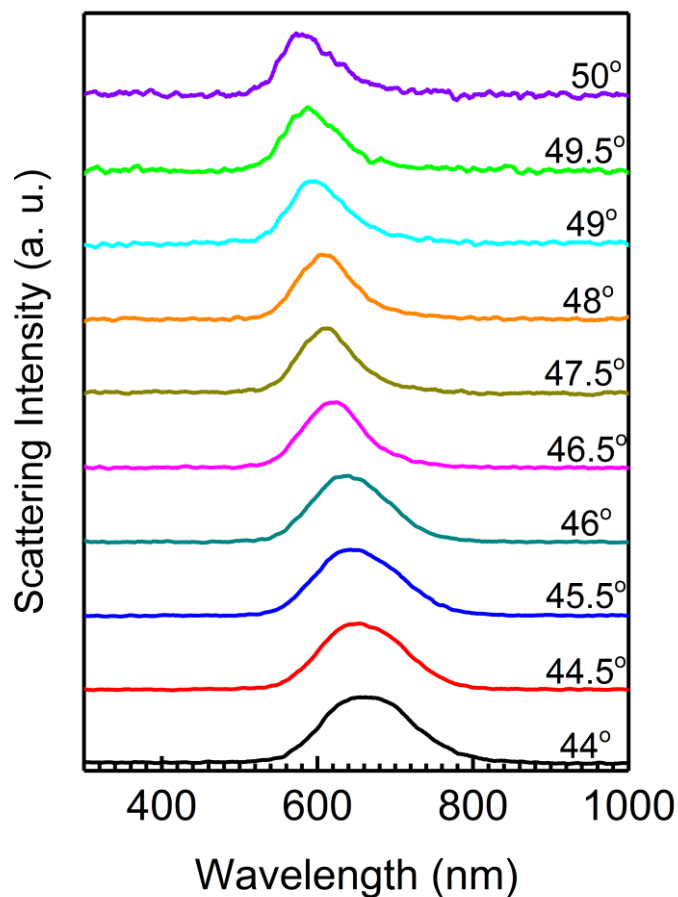

Figure S8. Scattering spectra measured for a plasmonic nanocavity (Ga nanoparticle + Au film) without an embedded WS$_2$ monolayer at different incidence angles.

S9: Normalized scattering spectra of Ga nanoparticles measured without Au film

The scattering spectra of Ga nanoparticles in the absence of the Au film are shown in Figure S9. It can be seen that the linewidth of the scattering spectrum of the Ga nanoparticle, which reflects the damping rate of the plasmons, is broadened dramatically to ~1105 meV in the absence of the Au film. It implies that the damping rate of the plasmons is increased significantly. In this case, the criterion for strong coupling, which is $\hbar\Omega > \dfrac{\gamma_{pl} - \gamma_{ex}}{2}$, is no longer fulfilled because of the large damping rate of the plasmons ($\hbar\Omega$ = 176 meV, γ_{pl} = 1105 meV, γ_{ex} = 33 meV). Therefore, the coupling is weak coupling when the Au film is absent.
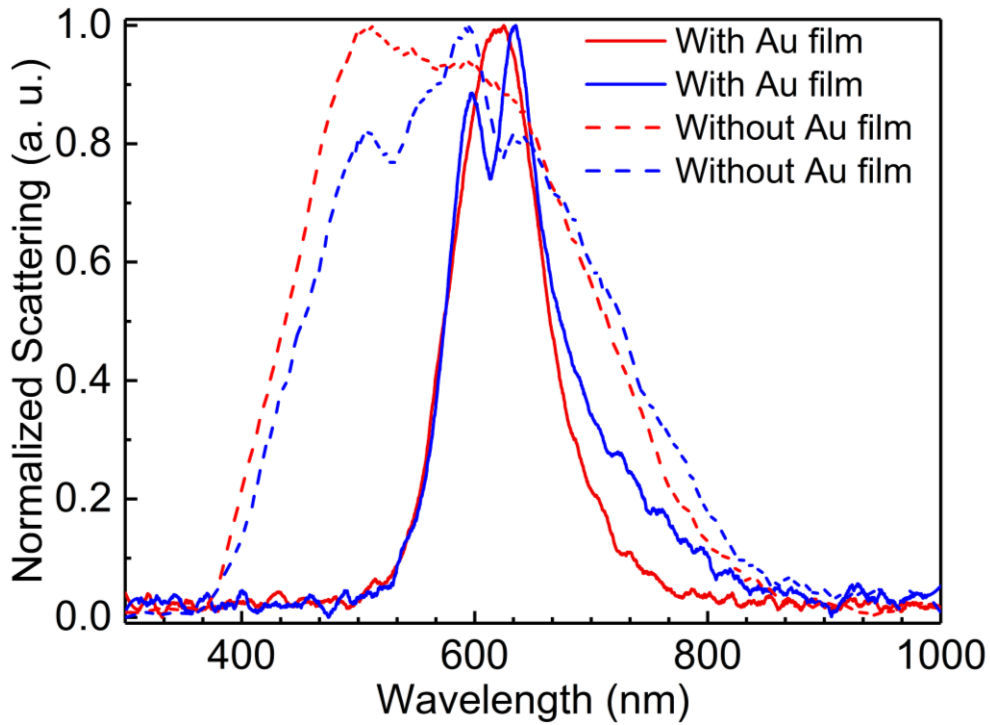

Figure S9. Normalized scattering spectra of Ga nanoparticles measured at an incidence angle of 46° under TM-polarized excitation. The red and blue curves correspond to the structures without and with WS_2 monolayer, respectively.